

Studies on Mechanical Properties and Morphology of Sisal Pulp Reinforced Phenolic Composites

SHIQI WANG

College of Materials Science and Engineering, Guilin University of Technology, Guilin 541004, People's Republic of China

CHUN WEI

Ministry-Province Jointly-Constructed Cultivation Base for State Key Laboratory of Processing for Non-Ferrous Metal and Featured Materials, Guangxi Zhuang Autonomous Region, Guilin 541004, People's Republic of China

HONGXIA LIU

Key Laboratory of New Processing Technology for Nonferrous Metals and Materials, Ministry of Education, Guilin 541004, People's Republic of China

YONGYANG GONG

College of Materials Science and Engineering, Guilin University of Technology, Guilin 541004, People's Republic of China

DEJIANG YANG, PENG YANG

College of Materials Science and Engineering, Guilin University of Technology, Guilin 541004, People's Republic of China

TIANXI LIU

Ministry-Province Jointly-Constructed Cultivation Base for State Key Laboratory of Processing for Non-Ferrous Metal and Featured Materials, Guangxi Zhuang Autonomous Region, Guilin 541004, People's Republic of China

Key Laboratory of New Processing Technology for Nonferrous Metals and Materials, Ministry of Education, Guilin 541004, People's Republic of China

College of Materials Science and Engineering, Guilin University of Technology, Guilin 541004, People's Republic of China

Correspondence to: Chun Wei; e-mail: 1986024@glut.edu.cn.

Received: November 19, 2014

Accepted: June 1, 2015

ABSTRACT: Based on renewable cellulosic resource, sisal pulp (SP) was prepared from wasted sisal fiber (SF) by the sulfate pulping method. The impact of the content of SP on the mechanical properties of phenolic composites was studied. For comparison, the reinforcement effect of SF, aramid pulp (AP), and glass fiber (GF) was studied. The microscopic structure and properties of the composites were characterized by polarized optical microscopy (POM), scanning electron microscopy (SEM), Dynamic thermomechanical analysis (DMA), and mechanical testing. Results show that the flexural strength and impact strength of SP-reinforced phenolic composites maximized at 125.6 MPa and 11.09 kJ/m², respectively, with 25wt% of SP. Compared with SF-, AP-, and GF-reinforced phenolic composites, the flexural strength of SP-reinforced phenolic composite has increased by 76.41, 25.35, and 14.29%, respectively, and impact strength increased by 49.26, 65.03, and 132.01%. POM illustrates that SP, SF, and AP subjected to a large shear during the roll milling process, and thus the fibers are cracked into finer microfibers. The results indicate that those microfibers and interfacial interaction affect reinforcement effect significantly. © 2015 Wiley Periodicals, Inc. *Adv Polym Technol* 2016, 35, 21557; View this article online at wileyonlinelibrary.com. DOI 10.1002/adv.21557

KEY WORDS: Composites, Impact resistance, Interfaces, Reinforcement, Sisal pulp

Contract grant sponsor: National Natural Science Foundation of China. Contract grant numbers: 21264005, 21204013, 51163003, and 51263005. Contract grant sponsor: Guangxi Natural Science Foundation of China. Contract grant num-

bers: 2013GXNSFDA019008 and 2014GXNSFAA118321. Contract grant sponsor: Foundation of Guangxi Ministry-Province Jointly-Constructed Cultivation Base for State Key Laboratory of Processing for Non-ferrous Metal and Featured Materials (13AA-6).

Introduction

Recently, burdened with the increasing environmental pollution, energy depletion, greenhouse effect and other issues, biomass material, an alternative of petrochemical resources, has drawn more and more attentions from researchers.^{1–5} Cellulose is a natural polymer material with advantages of largest reserves, environment-friendly, low costs, excellent mechanical properties, etc. It has been an extensively investigated as reinforcement for composites.^{1,2,4,6–9} Natural fibers have been used to partially replace glass fiber (GF), aramid pulp (AP), carbon fiber to reinforce the composites, and they have been applied in the interior parts of automotive and rail vehicles, etc.^{2,10–12}

Sisal is a tropical plant, belonging to Agavaceae. Sisal fiber (SF) has superior mechanical and antifriction properties, with tensile strength of 511–635 MPa and modulus of 9.4–22 GPa.^{1–7,12–15} Although GF-reinforced composites have satisfactory mechanical properties and applied widely, the density of GF is high. Meanwhile, during the process and usage, GF do great harm to the human body, which restrict its applications.^{3,10} AP and carbon fiber have good mechanical properties, but the cost is so high that they are only applicable in luxuries.¹⁶ Therefore, it is worthwhile to develop high-performance composites using natural plant fiber reinforced composites instead of GF.

Phenol formaldehyde (PF) resin is the first industrialized and an important resin, which has been used widely in automotive, aerospace, marine, electronics industries, etc.^{1,17–19} Nevertheless, the significant cross-linking density and brittleness of PF result in its low impact strength, and thus the reinforcement and toughening of it has been concerned.^{17–19} Using fibers to reinforce composites is an effective method, but the performance will be affected by fiber type, size, and the interfacial interaction. It has been reported that the size of fibers has a great influence on composites.^{20–22} When it comes to short fiber reinforced composites, a critical length of the fiber exists.^{23–26} If the fiber length is less than the critical value, the fiber will be extracted instead of breakage, regardless of the stress intensity. Consequently, the load bearing function of fiber cannot be fully utilized, resulting in poor reinforcement performance.^{27,28} Therefore, it is meaningful to clarify the respective impact of interfacial interaction, composites processing technology, and type of fiber on the properties of composites.

Using SF to reinforce PF has been investigated.^{9,11,19,29–33} However, there are wax and other chemicals on SF surface,^{8,33} resulting in a poor interfacial interaction with resin matrix. Numerous works on SF modification have been covered,^{9,11,19,29,31,33} such as alkali treatment, coupling agent treatment, surface grafting,¹¹ steam explosion treatment,³¹ and other methods. Megiatto and co-workers modified SF surface with treated lignin³³ and hydroxyl-terminated polybutadiene rubber¹⁹ to improve its bonding with PF interface. Botaro and co-workers¹¹ modified SF with NaOH and 3,3',4,4'-benzophenonetetracarboxylic dianhydride, but the modification effect is limited. There are plenty of hydroxyls in PF molecular chain, which can bond with the hydroxyls over natural fiber surface via hydrogen bonds.^{34,35}

Hence, based on this property, we prepared high-performance natural plant fiber reinforced PF composites through a simple method.

The previous works have focused on the interaction between SF and resin matrix, but the impact of processing technology on the morphology of SF is rarely studied. Typically, the composites of SF and PF are prepared and processed via solution mixing,^{19,32,33} in situ polymerization,⁹ roll milling and molding,³⁰ etc. During the roll milling process, fibers in PF matrix are subjected to mechanical shearing and crushing effect, resulting in the changes in morphology and size, which will affect its reinforcement effect. To compare the impact of machining processes on different types of fibers, we chose roll milling to prepare composites.

In this work, on the one hand, we used abandoned SF as a raw material to prepare sisal pulp (SP) via the sulfate-pulping process. During the processing, SP was further fibrillated into microfibers with a smaller diameter and larger length/diameter ratio. The influence of content, structure, and morphology on the mechanical properties of PF composites was investigated. On the other hand, SP/PF, SF/PF, AP/PF, and GF/PF composites were prepared by roll milling, grinding, molding, and other processes under the same processing conditions. The reinforcement and toughening effect of different types of fibers was compared and it laid the foundation for the application of natural fiber reinforced PF composites.

Experimental

MATERIALS

SF was supplied by Guangxi Sisal (People's Republic of China). AP (KP-5) was supplied by Shanghai Baibangcailiao (Shanghai, People's Republic of China). GF (E-glass) was purchased from Guangzhou Hetaisi Chemical (Guangzhou, People's Republic of China). PF (PF-8064) was supplied by Jinan Shengquan (People's Republic of China). Hexamethylenetetramine, sodium sulfide, sodium hydroxide, sodium chlorite, and acetic acid were analytically pure.

PREPARATION OF SP

SF was cut into short fibers with a length of 5 cm. SF (30.0 g), together with a solution comprising Na₂S (12.0 g), NaOH (12.0 g), and distilled water (300 mL), was added to a 500-mL high pressure reactor, which was placed in a thermostatic oven to react at 170°C for 3 h. After filtration, the filtrate was collected for posttreatment and rinsed with deionized water and dried; 20.0 g of the product was added to a 1000-mL three-necked flask, mixed with a solution composed of NaClO₂ (6.0 g), acetic acid (5.0 mL), and distilled water (650 mL). The reaction proceeded for 1 h at 80°C. Then, NaClO₂ (6.0 g) and acetic acid (5.0 mL) were added to commence further reaction for 1 h. Then, it was washed with deionized water. The residual was then dried to obtain SP. The entire SP preparation process is illustrated in Fig. 1.

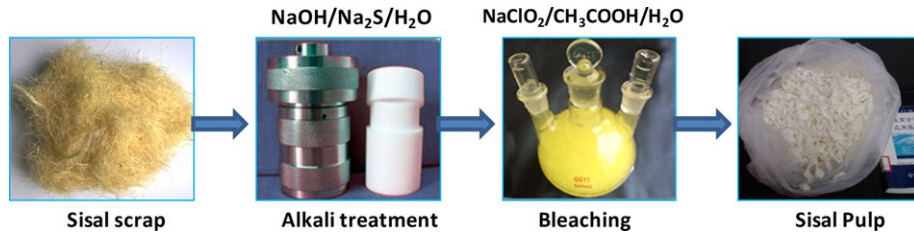


FIGURE 1. Preparation process of SP.

TABLE I
Materials of SP/PF Composites

Content of Fiber (wt%)	SP (g)	PF (g)	Zinc Stearate (g)	HMTA (g)
0	0.0	90.0	1.8	9.0
10	9.0	81.0	1.8	8.1
20	18.0	72.0	1.8	7.2
30	27.0	63.0	1.8	6.3
40	36.0	54.0	1.8	5.4

TABLE II
Formulas of Different Types of Fiber-Reinforced PF Composites

Type of Fiber	Fiber (g)	PF (g)	Zinc Stearate (g)	HMTA (g)
SP	22.5	67.5	1.8	6.8
SF	23.0	47.0	1.4	4.7
AP	22.7	75.0	2.0	7.5
GF	41.3	75.0	2.0	7.5

PF, phenol formaldehyde; HMTA, hexamethylenetetramine.

PREPARATION OF PF COMPOSITES

According to the formulation described in Tables I and II, raw materials were prepared to manufacture PF composites. The fiber, PF, zinc stearate, and curing agent were added to a high-speed grinder for mechanical crushing and blending for 1 min until SF was uniformly mixed with resin. The mixture was processed with a roller mill (temperature of two rolls was 120 and 100°C, respectively) for 10 min. After cooled to ambient temperature, it was crushed using a high-speed grinder to obtain PF composites. Then, the specimens with dimensions of about 4.0 mm thick, 80.0 mm long, and 10.0 mm wide were manufactured after placing in a mold for 5 min at 165–170°C with 50–60 MPa. Finally, the specimens were postcured at 120, 140, 160, and 180°C for 3 h. The preparation process of PF composites is illustrated in Fig. 2. and materials of SP/PF composites are presented

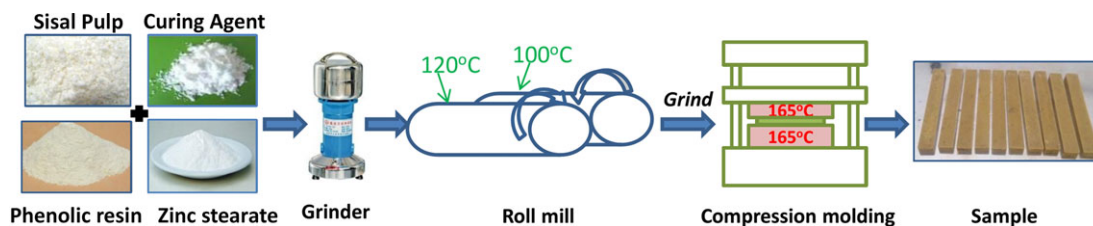


FIGURE 2. Preparation process of PF composites.

in Table I. The formulation of different types of fiber-reinforced PF composites is presented in Table II.

CHARACTERIZATION AND TESTING

An AJSM-6380 LV scanning electron microscope was used to characterize the morphology of fracture surface, which was painted with a thin layer of gold. Thermogravimetric analysis (TGA) was carried out with a TA Q500 device with a heating rate of 10°C/min in N₂ flow from 50 to 800°C. A polarized optical microscope (Nikon ECLPSE E200) with a hot stage was used to observe the morphology of the composites. The Charpy impact testing was performed on a JC-25 tester, using rectangular bar specimens with dimensions of about 4.0 mm thick, 80.0 mm long, and 10.0 mm wide, in accordance with the standard GB 1043-93. More than 10 specimens were tested to obtain the average value. Three-point bending test was performed on a WDW-20 computer-controlled electronic universal testing machine at a pressing speed of 2 mm/min and a gauge length of 64 mm in accordance with the standard GB T9341-2008. More than five specimens with a size of 4.0 mm thick, 80.0 mm long, and 10.0 mm wide were tested, and the mean was calculated to represent the real value. DMA was carried out with a TA Q800 device at single cantilever mode with a heating rate of 3°C/min in air flow from 30 to 300°C. The maximum force and amplitude were set at 1 N and 1 μm, respectively. The dimensions of specimens were 4.0 mm thick, 35.0 mm long, and 10.0 mm wide.

Results and Discussion

MECHANICAL PROPERTIES

Effect of the Content of SP

Generally, for fiber-reinforced composites, the effect of the content of fiber on the mechanical properties of the composites

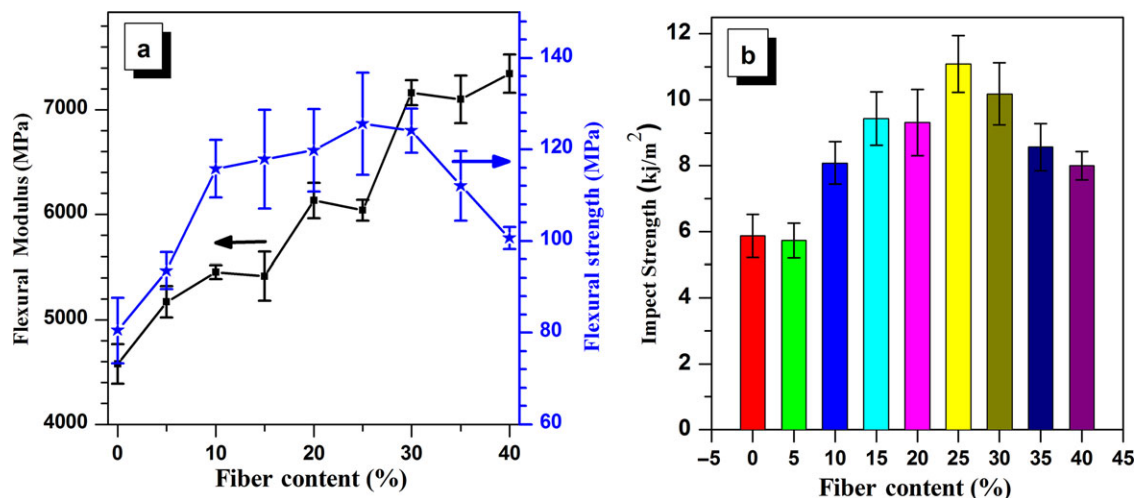


FIGURE 3. (a) Flexural strength and (b) impact strength of PF composites with different content of SP.

is more significant.^{1,3,9} So, it is worth studying the impact of the mass fraction of SP on performance of PF composites. Flexural strength and impact strength of PF composites with different content of SP are depicted in Fig. 3. As can be seen from Fig. 3a, with an increase in SP, the flexural strength of SP/PF composites increased first and then decreased. The flexural strength maximized (125.6 MPa) at 25 wt% of SP, higher than that of pure PF composite by 56%. It implied that with the increase in the content of fiber, the amount of stress delivering fibers in the same cross-sectional area of the composites increases, so the stress-bearing capability thereby enhanced. The material becomes rigid and strong, and the flexural strength and modulus increase. However, with a further increase in fiber, the volume fraction of fiber in the composites increases, so the relative mass fraction of resin reduces. Accordingly, the amount of defects inside the composites increases, resulting in a decreased flexural strength of the material. Hence, the flexural strength (100.6 MPa) of the composites with 40 wt% of SP is lower than that of the composites with 25wt% of SP by 20%.

Unlike tensile and flexural properties of composites, impact property is the resistance capability of crack initiation and crack expansion of composites under high-speed impact.²⁸ It is relevant to fiber type, content, arrangement of fibers, interfacial properties, and so on. Impact energy is dissipated by the fracture of fibers or matrix and extraction of fibers.^{3,36} The result from Fig. 3b shows that, with the increase in the content of SP, the impact strength of SP/PF composites increases at first and then decreases. When the content of fiber is 25 wt%, impact strength of the composite reaches a maximum of 11.09 kJ/m², higher than that of pure PF by 189%. However, when the content of fiber is up to 40 wt%, the impact strength of composite (8.00 kJ/m²) declines by 28% than that of the above (25 wt% of SP). This is analogous to the case of flexural strength.

Effect of the Types of Fibers

The effect of different types of fibers on composites was affected by their natures, interfacial bonding conditions, and other

factors. On the same condition of fiber volume fraction of 20.4% (corresponding to the SP/PF composites with 25 wt% of SP), SF/PF, SP/PF, AP/PF, and GF/PF composites were prepared to investigate their mechanical properties.

Flexural strength and impact strength of different types of fiber-reinforced PF composites are depicted in Fig. 4. In Fig. 4a, under the conditions of same volume fraction and same processing, molding, and curing parameters, the flexural strength of SF/PF, SP/PF, AP/PF, and GF/PF composites is 71.2, 125.6, 100.2, and 109.9 MPa, respectively, and the specific strength (as in Table III) is 56.96, 96.62, 78.28, and 72.78 MPa/(g/cm³), respectively. It is concluded that the reinforcement effect of SP on PF is optimal and greater than that of SF/PF, AP/PF, and GF/PF composites by 76.41%, 25.35%, and 14.29%, respectively. It may attribute to the appropriate size and length/diameter ratio of SP, and the favorable interaction between SP and matrix.

It is shown in Fig. 4b that the impact strength of SF/PF, SP/PF, AP/PF, and GF/PF composites is 7.43, 11.09, 6.72, and 4.78 kJ/m², respectively. The SP/PF composite has the optimal impact properties, which are higher than those of SF/PF, AP/PF, and GF/PF composites by 49.26%, 65.03%, and 132.01%. This is attributed to that cellulose, the component of SP, has a large number of hydroxyls on its surface. Hence, hydrogen bonds will be formed between these hydroxyls and the hydroxyls of PF,^{34,35} and resulting in the favorable interfacial interaction.

The dependence of storage modulus (E'), internal friction ($\tan \delta$) of the neat PF, and four types of composites on the temperature is shown in Fig. 5. The glass transition temperatures (T_g) from onset of the drop in storage modulus (use tangent method) and $\tan \delta$ peak of the neat PF and its composites are presented in Table IV. The effect of addition of fibers on the composites storage modulus is very pronounced in the studied temperature range as presented in Fig. 5a. Results show that the sequence of the E' s from high to low is as follows: GF/PF, AP/PF, SP/PF, SF/PF, and PF within the glassy region. This is in agreement with the static flexural modulus of composites. The E' s of both PF and its composites decreased rapidly near 192°C, which correspond to the glass transition (see in Table IV). For polymer composites, the change in T_g is raised by the physical or chemi-

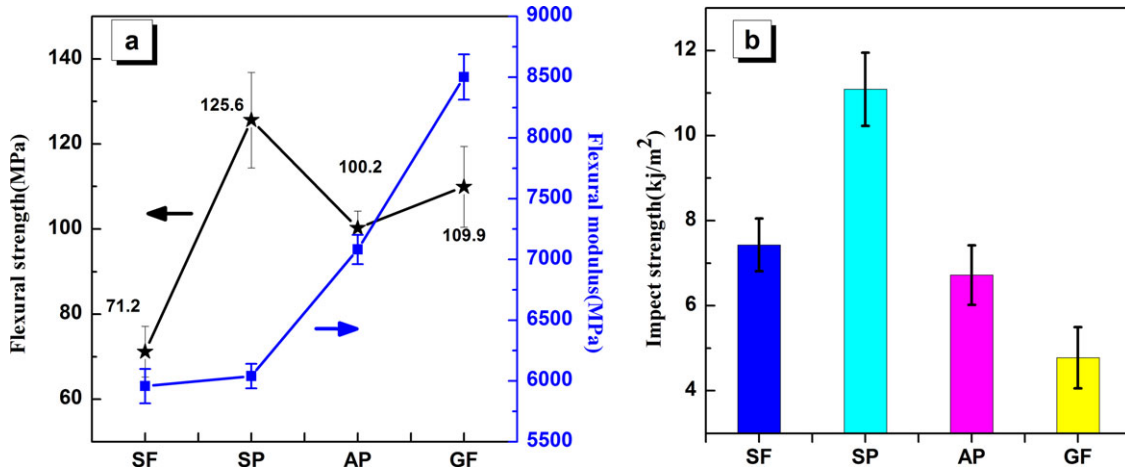


FIGURE 4. Effect of different types of fibers on (a) flexural strength and (b) impact strength of PF composites.

TABLE III
Density and Specific Strength of Fibers and Their Composites

Fiber	Fiber Density ^a (g/cm ³)	Fiber/PF Density ^a (g/cm ³)	Specific Strength of Composites (MPa/(g/cm ³))
SF	1.47	1.25	56.96
SP	1.58	1.30	96.62
AP	1.43	1.28	78.28
GF	2.60	1.51	72.78

^aThe density of fibers and composites was measured by Archimedes (with the use of water as an immersion fluid).

TABLE IV
Glass Transition Temperatures of Neat PF and Its Composites Determined by Onset of Storage Modulus Drop and Peak of Tan δ

	PF	SF/PF	SP/PF	AP/PF	GF/PF
$T_g (E')$ (°C)	192.53	196.50	194.24	191.64	192.62
$T_g (\tan \delta)$ (°C)	227.35	227.20	230.28	230.28	231.66

cal confinement of polymer chains, which is usually caused by a strong interaction between the polymer matrix and the reinforcing fibers.^{25,33} So, the $T_g (E')$ and $T_g (\tan \delta)$ are slightly shifted to high temperature after the addition of fibers.

Tan δ is a measurement of viscoelastic damping of materials. From the tan δ curve (in Fig. 5b), the neat PF has a high tan δ value because there is no restriction to the chain motion. After the addition of fibers, the rigid fillers reduced the polymer chain mobility, and the height of the tan δ peak decreases significantly. The lower tan δ peak after the addition of fillers indicates that the composites become more elastic and less energy is dissipated during mechanical vibrations. The result shows that the sequence of the height of the tan δ peak from high to low is as follows: PF, SF/PF, AP/PF, GF/PF, and SP/PF. As SP/PF composite, smaller values of tan δ indicate better interaction in the fiber/matrix interface, because the improvement in the composite interface might lead to a more efficient stress transfer between the fibers and matrix, and lower energy dissipation, consequently decreasing tan δ . Furthermore, to find out other factors that affect the mechanical behavior of composites, we studied the morphologies of fibers and their composites.

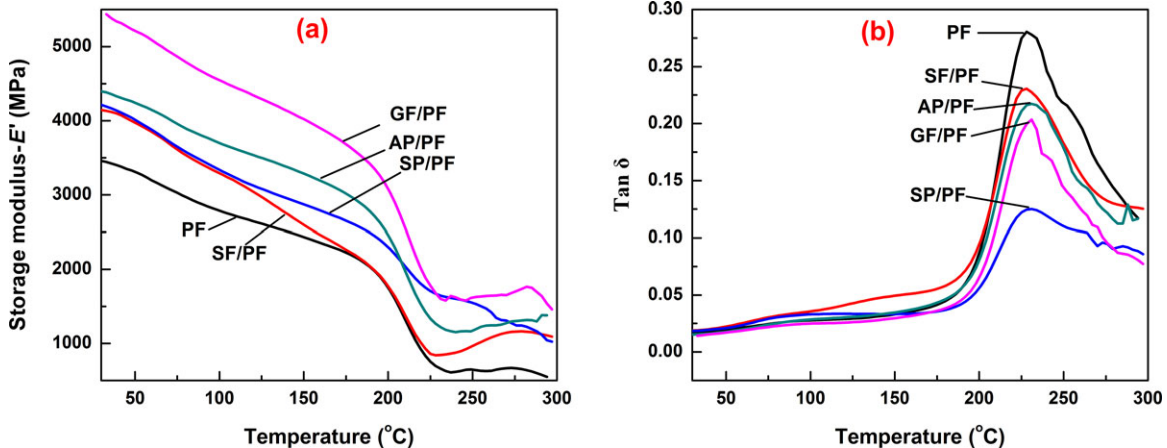


FIGURE 5. Dynamic mechanical properties of neat PF and four types of composites: (a) storage modulus and (b) tan δ .

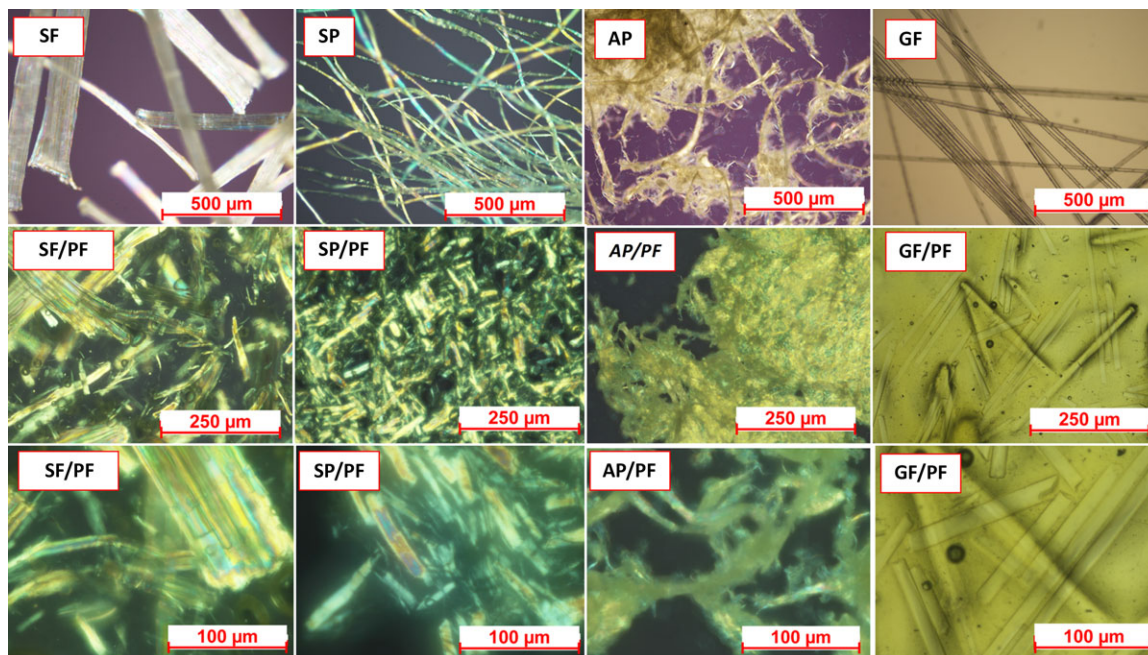


FIGURE 6. POM photographs of the fibers and their composites (photos of GF and GF/PF were taken under natural light).

MORPHOLOGIES OF FIBERS AND THEIR COMPOSITES

For a short fiber reinforced polymer composite, fiber size has a great influence on the properties of composite.^{20,27,28,37} Polarized optical microscopy (POM) images of different types of fibers and their composites are shown in Fig. 6. It is observed that the diameters of SF, SP, and AP fibers are uneven, whereas the diameters of GF are relatively uniform. The average diameter of SF, SP, AP, and GF is 68.8, 13.1, 14.1, and 12.3 μm , respectively (average the diameters of 50 fibers in the microscopy images). Moreover, the surface of SF, SP, and GF fiber is smooth, whereas there are numerous fine fibers distributed on the surface of AP fibers. This is due to aramid fiber subjected to mechanical crushing during the preparation process and fibrillation to form AP.

Comparing the microscopic morphologies of fibers in SF/PF, SP/PF, AP/PF, and GF/PF composites with the original fibers, it can be seen that the diameter of fibers varies little but the length changes evidently. The average lengths of SF, SP, AP, and GF are 166.3, 66.1, 379.0, and 318.4 μm , respectively, and the average diameters are 39.0, 10.1, 13.5, and 12.3 μm . Thus, the length/diameter ratios are 4.3, 6.6, 28.1, and 25.9. As a result, under the same processing conditions, the average lengths of SF and SP were significantly reduced from centimeters to 166.3 and 66.1 μm , respectively. These fibers subjected to shearing during the roll milling and grinding processing result in fracture and peeling off from the fibers, and these fibrils were split into smaller microfibrils. However, the above behaviors never occurred in the case of GF/PF. This is due to the GF because it is an isotropic material and has no microfibrillar structure. As shown in the images of AP/PF, AP fibers are subjected to shear during the processing, and the resin adheres on it by melting. Accordingly, the AP surface became smooth and the fibrillated fibers on the surface disappeared. Evaluated from the microscopic

images, the average diameter of the microfibrils in SF/PF, SP/PF, and AP/PF composites is 5.0, 2.4, and 3.5 μm , respectively, and the average lengths are 41.4, 26.2, and 47.1 μm , respectively.

In terms of observed morphology, dispersion of fiber in composites, and its interfacial interaction with resin matrix, the scanning electron microscopy (SEM) images of the impacted fracture sections of SF/PF, SP/PF, AP/PF, and GF/PF composites are shown in Fig. 7. Diameters of the SF, SP, AP, and GF fiber in the composites are 37.0, 9.6, 14.6, and 13.9 μm , respectively, which agree well with the results obtained by POM. In the subimage of SF/PF, the extraction surface of SF fiber is smooth and the debonding between the fibers and resin takes place, indicating the poor compatibility between SF and PF and resulting in the poor mechanical properties of SF/PF. The pull out of fibers also show in the SP/PF, AP/PF, and GF/PF composites. The extraction surface of GF/PF is smoothest, proving that GF has poor interfacial interaction with the resin matrix. The SP fibers were rarely extracted, reflecting the intensive interfacial adhesion between SP and the resin matrix. It is in agreement with the results obtained by DMA, which may result in formation of hydrogen bond between hydroxyls (-OH) on the surface of SP and PF. Therefore, the SP/PF composite has better mechanical properties than the other three.

Based on the fracture section morphologies of GF/PF and the other three shown in Fig. 7, only the fracture section of GF/PF composite is flat and smooth (labeled with a circle in Fig. 7 of GF/PF), whereas the fracture surfaces of SP/PF, AP/PF, and SF/PF are rough. It may be attributed to shearing of SF, SP, and AP during the processing, resulting in the fiber breakage and cracking into fine microfibrils (Fig. 6). These microfibrils are uniformly dispersed in the resin to reinforce the composites and lead to the dissipation of impact energy. Nonetheless, such an effect has not been observed for GF, so its fracture section is flat and smooth and impact performance is poor.

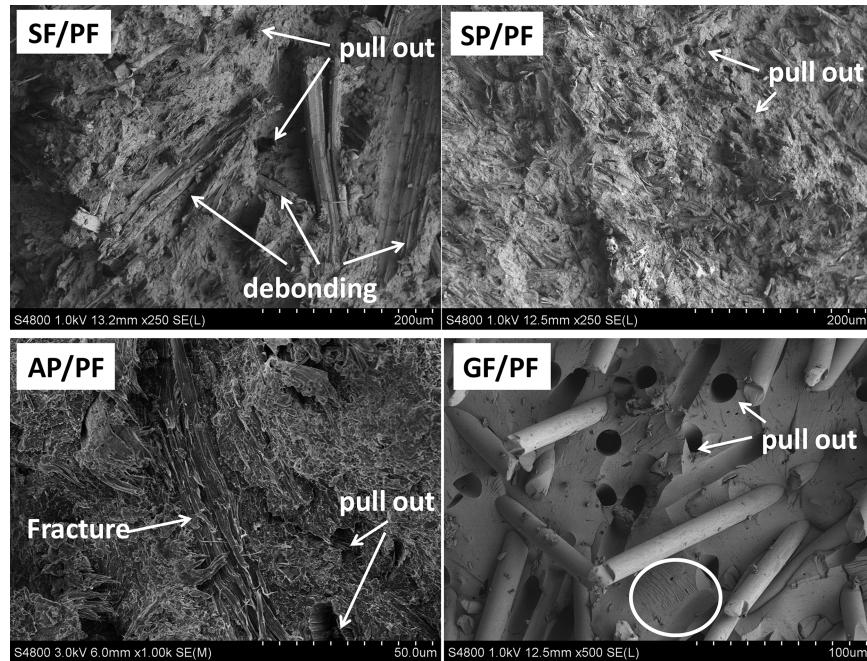


FIGURE 7. SEM images of impacted fracture sections for four types of composites.

TABLE V
Thermal Decomposition Results of SP/PF Composites Based on TGA

SP Content (%)	$T_{d_5}^a$ (°C)	T_{max}^a (°C)	Char Yield (%)
0	406.42	449.5	64.09
10	334.92	352.00	56.30
20	325.17	351.98	52.29
30	314.05	350.50	43.02
40	308.58	349.70	40.37

^a T_{d_5} refers to the temperature at which 5% of a material decomposes; T_{max} is the temperature to which maximum decomposition rate corresponds.

Simultaneously, in SF/PF composites, prepared by the solution mixing method,^{32,34,35} due to the absence of strong mechanical shear action, SF cannot break and crack into fine microfibers. Therefore, the SEM image is similar to that of GF/PF composites. It implies that the microfibers generated from the processing contribute significantly to the reinforcement on composites.

THERMAL STABILITY OF FIBERS AND THEIR COMPOSITES

Thermal stability is an important indicator of composites, which limits its application. TGA curves for the composites with different SP contents are depicted in Fig. 8a, and resultant analysis is presented in Table V. It illustrates that with the increase in SP, T_{d_5} of the SP/PF composites decreases gradually. Because of the thermal decomposition, temperature of SP is lower than the PF. In the TGA curves of SP and SP/PF, the thermal decomposition at the first stage is attributed to the decomposition of cellulose, which is the compound of SP.^{34,35,38} Simultaneously,

TABLE VI
TGA Results of Fibers and Their Composites

Sample	T_{d_5} (°C)	T_{max} (°C)	Char Yield (%)
SF	261.08	284.00/345.40	24.00
SP	298.18	342.90	18.62
GF/PF	421.20	445.75	74.16
AP/PF	397.70	445.75/530.45	51.50
SP/PF	318.65	349.70	48.58
SF/PF	296.35	344.42	49.18

it is illustrated in Table V that the char yield of composites is gradually decreased with the addition of SP, which is also due to the lower char yield of SP.

TGA curves of different types of fiber-reinforced PF composites are shown in Fig. 8b, and the result is presented in Table VI. It is noted that the T_{d_5} of GF/PF, AP/PF, SP/PF, and SF/PF is 421.20, 397.70, 318.65, and 296.35°C, respectively, indicating SP/PF and SF/PF have poor thermal stability. Compared with SF and SF/PF, the T_{d_5} of SF/PF is higher than that of SF by 35.27°C. It may be attributed to PF coating, improving thermal stability.

Conclusions

In summary, SP/PF composites were studied and the reinforcement effect of SP was compared with SF, AP, and GF. First, with the increase in the content of SP, the flexural strength and impact strength of SP/PF composites increase at first and then

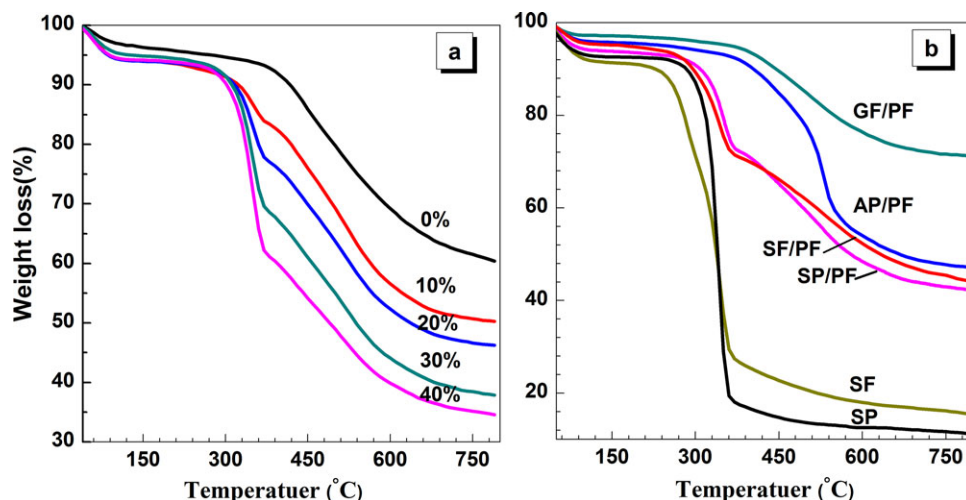


FIGURE 8. TGA curves of the composites: (a) with different content of SP and (b) with different types of fibers.

decrease. Second, the morphologies of different types of fibers and their composites illustrate that SP, SF, and AP are subjected to a large shear during the roll milling process, and thus these fibers are cracked into finer microfibrils. But, it will not take place in GF. The SEM images of impacted fracture sections for different types of fiber-reinforced PF composites show that microfibrils affect the morphologies of impacted fracture sections greatly, and both the microscopic structure of fiber and interfacial interaction affect the mechanical properties of composites significantly.

References

- Thakur, V. K.; Thakur, M. K. *Carbohydr Polym* 2014, 109, 102.
- Faruk, O.; Bledzki, A. K.; Fink, H.-P.; Sain, M. *Prog Polym Sci* 2012, 37, 1552.
- Wambua, P.; Ivens, J.; Verpoest, I. *Compos Sci Technol* 2003, 63, 1259.
- Rukmini, K.; Ramaraj, B.; Shetty, S. K.; Taraiya, A.; Bandyopadhyay, S. *Siddaramaiah. Adv Polym Technol* 2013, 32, 21327.
- Rana, A. K.; Singha, A. S. *Adv Polym Technol* 2014, 33, 21433.
- Kong, C.; Park, H.; Lee, J. *Mater Lett* 2014, 130, 21.
- Xie, Y. J.; Hill, C. A. S.; Xiao, Z. F.; Militz, H.; Mai, C. *Composites, Part A* 2010, 41, 806.
- Kabir, M. M.; Wang, H.; Lau, K. T.; Cardona, F. *Composites, Part B* 2012, 43, 2883.
- Mu, Q.; Wei, C.; Feng, S. *Polym Compos* 2009, 30, 131.
- Holbery, J.; Houston, D. *JOM* 2006, 58, 80.
- Botaro, V. R.; Siqueira, G.; Megiatto, J. D.; Frollini, E. *J Appl Polym Sci* 2010, 115, 269.
- Ku, H.; Wang, H.; Pattarachaiyakooop, N.; Trada, M. *Composites, Part B* 2011, 42, 856.
- Bledzki, A. K.; Gassan, J. *Prog Polym Sci* 1999, 24, 221.
- Mohan, T.; Kanny, K. *Composites, Part A* 2012, 43, 1989.
- Saheb, D. N.; Jog, J. P. *Adv Polym Technol* 1999, 18, 351.
- Choi, M. H.; Jeon, B. H.; Chung, I. *J Polym* 2000, 41, 3243.
- Taylor, J. G. In *Phenolic Resins: A Century of Progress*; Pilato, L. (Ed.); Springer: Heidelberg, Germany, 2010; Vol. 3, pp. 263–269.
- Gardziella, A.; Pilato, L. A.; Knop, A. In *Phenolic Resins: Chemistry, Applications, Standardization, Safety and Ecology*; Gardziella, A.; Pilato, L. A.; Knop, A. (Eds.); Springer: Heidelberg, Germany, 2000; Vol. 2, pp. 75–77.
- Megiatto, J. D. Jr; Ramires, E. C.; Frollini, E. *Ind Crop Prod* 2010, 31, 178.
- Nakagaito, A. N.; Yano, H. *Appl Phys A* 2004, 78, 547.
- Xu, X. Z.; Liu, F.; Jiang, L.; Zhu, J. Y.; Haagenson, D.; Wiesenborn, D. P. *ACS Appl Mat Interfaces* 2013, 5, 2999.
- Rusli, R.; Shanmuganathan, K.; Rowan, S. J.; Weder, C.; Eichhorn, S. J. *Biomacromol* 2011, 12, 1363.
- Bowyer, W. H.; Bader, M. G. *J Mater Sci* 1972, 7, 1315.
- Fu, S.-Y.; Lauke, B. *Compos Sci Technol* 1996, 56, 1179.
- Du, Y. C.; Wu, T. F.; Yan, N.; Kortschot, M. T.; Farnood, R. *Composites, Part B* 2014, 56, 717.
- Zhu, H.-H.; Zhang, C.-C.; Tang, C.-S.; Shi, B.; Wang, B.-J. *Geotext Geomembranes* 2014, 42, 329.
- Du, S. Y.; Wang, B. In *Mesomechanics of Composites*; Du, S. Y.; Wang, B. (Eds.); Science Press: Beijing, People's Republic of China, 1998; Vol. 4, pp. 118–160.
- Zeng, X. R. In *Micromechanical Properties of Composites*; Qiao, S. R., (Ed.); Northwestern Polytechnical University Press: Xi'an, People's Republic of China, 1997; Vol. 4, pp. 52–62.
- Yang, G. C.; Zeng, H. M.; Li, J. J. *Fiber Reinf Plast/Compos* 1997, 3, 12.
- Wei, C.; Zeng, M.; Xiong, X. M.; Liu, H. X.; Luo, K.; Liu, T. X. *Polym Compos* 2015, 36, 433.
- Zhong, J. B.; Niu, Y. L.; Lu, J.; Wei, C. *China Plast Ind* 2006, 34, 53.
- Megiatto, J. D. Jr; Silva, C. G.; Ramires, E. C.; Frollini, E. *Polym Test* 2009, 28, 793.
- Megiatto, J. D. Jr; Silva, C. G.; Rosa, D. S.; Frollini, E. *Polym Degrad Stab* 2008, 93, 1109.
- Faulstich de Paiva, J. M.; Frollini, E. *Macromol Mater Eng* 2006, 291, 405.
- Ramires, E. C.; Megiatto, J. D., Jr.; Gardrat, C.; Castellan, A.; Frollini, E. *Biore-sour Technol* 2010, 101, 1998.
- Graupner, N.; Rößler, J.; Ziegmann, G.; Müssig, J. *Composites, Part A* 2014, 63, 133.
- Wong, S.-C.; Baji, A.; Leng, S. *Polymer* 2008, 49, 4713.
- Benítez-Guerrero, M.; López-Beceiro, J.; Sánchez-Jiménez, P. E.; Pascual-Cosp, J. *Thermochim Acta* 2014, 581, 70.